Jurnal Elektronika dan Telekomunikasi (JET), Vol. 25, No. 2, December 2025, pp. 80- 85
Accredited by KEMDIKBUDRISTEK, Decree No: **158/E/KPT/2021**
doi: 10.55981/jet.679

2.4 GHz Energy Harvester for Ultra-Low Power IoT Sensor Applications

Farrah Vauzia[a,*], Enceng Sulaeman[a], Yana Taryana[b]

[a]Electrical Engineering Department
Politeknik Negeri Bandung
Jl. Gegerkalong Hilir, Ciwaruga
Bandung, Indonesia
[b]Research Center for Telecommunications
National Research and Innovation Agency
Jl. Sangkuriang, Dago,
Bandung, Indonesia

Abstract

IoT is a technology that integrates various devices and can be controlled remotely via the internet. Currently, IoT is rapidly developing in sectors such as health, agriculture, housing, and more. Sensors play an essential role in IoT devices to collect information from the surrounding environment. The sensors rely on batteries as a power source, which affects their performance. Recent technologies have developed ultra-low power sensors to extend the battery life. However, using batteries for IoT devices over a long period is not cost-effective and efficient in terms of installation. To address this issue, an Energy Harvester system has been developed. This system collects energy from the surrounding environment and converts it into electrical energy. The focus of this research is to design and implement an energy harvester powered by Radio Frequency (RF), specifically in the 2.4 GHz frequency band for ultra-low power IoT sensor applications. The RF energy harvester (RFEH) was designed and simulated using ADS 2011.11 software. The RFEH was fabricated on FR4 epoxy PCB and the measurement was conducted in two conditions: directly connected to the signal generator and in a far-field area. The harvester achieved a maximum output current of 32.6 µA under a received power of -3 dBm, satisfying the requirements for ultra-low power IoT sensors.

Keywords: Energy harvester, IoT, 2.4 GHz, RF-DC Converter, Rectenna

I. INTRODUCTION

Internet of Things (IoT) technology is growing rapidly along with society's needs. IoT technology enables users to control devices remotely through an internet connection. To be interconnected with various devices, an IoT system consists of sensors, power sources, transceivers, and processors [1]. Sensors play an essential role in collecting information from the surrounding environment, such as humidity, heat, distance, and so on. In many instances, sensors are located in remote and inaccessible areas, requiring batteries as a power source for operation. Hence, regular maintenance and battery replacement are necessary [2] [3]. Battery-powered systems not only demand frequent maintenance but also increase operational costs and complexity in large-scale deployments.

To address these challenges, ultra-low power IoT sensors have been developed by reducing current consumption to extend battery life [4]-[6]. To preserve energy, most IoT devices remain in sleep mode for most of the time [7]. The current consumption is as low as 1 to 10 µA in sleeping mode and 5 to 10 mA for communication [8]. The low-power applications only require received power at about 1 mW [9].

* Corresponding Author.
Email: farrah.vauzia@polban.ac.id
Received: September 10, 2024 ; Revised : November 18, 2024
Accepted: May 23, 2025 ; Published: December 31, 2025

However, relying solely on batteries remains inefficient for sustainable IoT applications. Although power consumption is low, battery replacement is still required. Therefore, an energy harvester was developed. Radio frequency (RF) is a significant energy source due to its widespread use and easy accessibility [10]. An RF Energy Harvester (RFEH) is shown in Figure 1. RF signals from the surroundings are received by the antenna and then rectified by an RF to DC rectifier that generates a constant DC voltage [11],[12]. To optimize the power received by the system, a matching impedance circuit must be inserted between the antenna and the rectifier.

However, the voltage generated from the matching impedance is typically too low to overdrive the diode in the RF-to-DC rectifier. Therefore, an RF-to-DC rectifier circuit should be carefully designed [13] by selecting the appropriate topology and components. There are several commonly used topologies for RF-to-DC converters, such as Dickson, Villard, and Greinacher [14].

In this research, we designed, fabricated, and tested a Radio Frequency (RF) energy harvester optimized for ultra-low-power IoT sensors, targeting the 2.4 GHz frequency band. The primary objective was to develop an

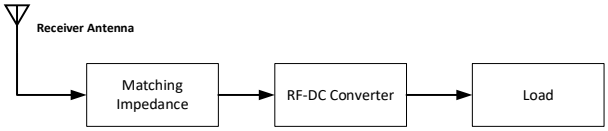

Figure 1. RF Energy Harvesting System Block Diagram.

RF energy harvester that operates efficiently at 2.4 GHz, specifically tailored to meet the energy demands of ultra-low-power IoT sensor applications. Schottky diodes were employed in the Greinacher RF-DC topology due to their low forward voltage characteristics and are suitable for use in low-power systems [15]. The proposed design extends the sensitivity to -20 dBm with a load resistance of 1 kΩ. In the experiment, far field sensitivity at certain distances was also performed.

By harvesting ambient RF energy more effectively, the findings contribute to the development of self-sustaining IoT devices, reducing dependence on traditional power sources and advancing the field of energy-efficient wireless technology.

II. METHODS

A. Circuit Topology Selection

The main part of RFEH is the rectifier that converts RF signals to DC voltage. RF signals are formed in sinusoidal waves in a high-frequency range. A rectifier circuit may consist of diodes, transistors, or CMOS arranged in certain ways [3],[11]. Figure 2(a) shows the basic half-wave rectifier circuit, where the output is a DC signal with ripples. To smooth out the ripples and form a completely flat DC signal, capacitors are added to the circuit as in Figure 2(b).

When designing rectifier circuits, it is important to consider factors such as low power consumption, increased power sensitivity, and good power processing capacity. In the UHF range, the input power received by the antenna is typically less than 0 dBm [16],[17]. In other words, the input voltage is very low, so it needs to be increased to obtain the DC output voltage. To boost the DC output voltage, rectifiers are used in multiple stages to multiply the input voltage [18]. Several voltage multiplier configurations, such as Dickson, Villard, and Greinacher, were compared in [19]. For all input parameters, such as input power and input frequency, the Greinacher voltage multiplier has the highest efficiency

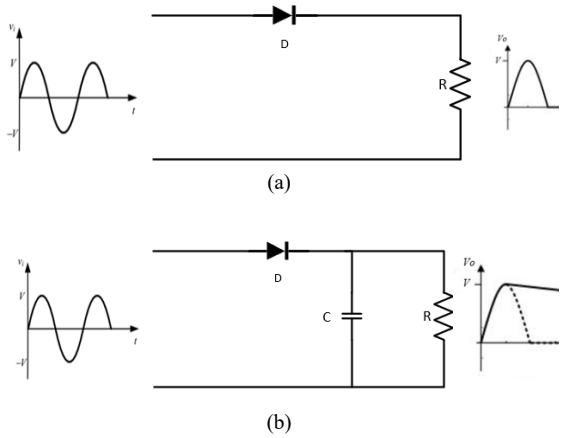

Figure 2. (a) Half-wave rectifier circuit (b) Half-wave rectifier with filter.

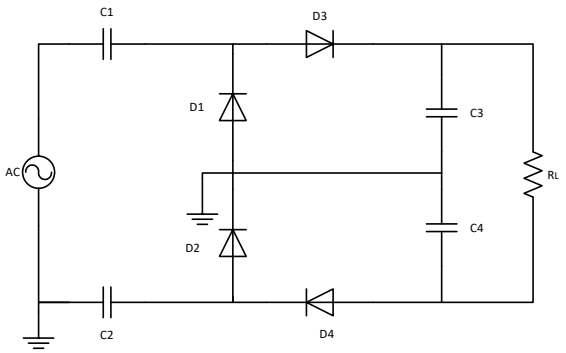

Figure 3. Greinacher Topology.

of 25% at 0 dBm input power among other configurations.

Figure 3 is the Greinacher voltage multiplier topology which is a cascaded multiple half-wave rectifier. The output DC voltage is given by (1).

$$V_{dc} = 2nV_m \quad (1)$$

where V_m is the maximum input voltage and n is the number of the rectifier stages [20].

B. Component Selection

The diode has the main role in the rectifying process; hence, it should be chosen carefully. Unlike other types of diodes, the Schottky diode uses only one type of semiconductor material, p-type or n-type, and is connected to a metal. The Schottky diode has a low forward voltage drop that results in a faster switching response compared to other diodes. Therefore, it is suitable to work at high frequency [21].

Among various types of Schottky diodes, HSMS 2860 is selected. It has a frequency range of 915 MHz to 5.8 GHz that covers the proposed RFEH frequency of 2.4 GHz. The SPICE parameters are given in the datasheet provided by Avago in Table 1.

Four HSMS 2860 chips are used in the Greinacher topology because it only contains a single diode. After configuring the circuit, the above parameters were

TABLE 1
HSMS 2860 SCHOTTKY DIODE CHARACTERISTICS

Parameter	Value
Frequency	915 MHz to 5.8 GHz
Forward Voltage (V_f)	250 mV to 350 mV
Reverse breakdown voltage (B_v)	7 V
Zero-bias Junction capacitance (C_{J0})	0.18 pF
Energy gap (E_G)	0.69 eV
Current at reverse breakdown voltage (I_{BV})	10 µA
Saturation Current (I_s)	50 nA
Emission Coefficient (N)	1.08
Ohmic Resistance (R_s)	6 Ω
Junction Potential (VJ)	0.65 V
Saturation-current temperature exponent (XTI)	2
Grading Coefficient (M)	0.5

modelled for simulation. The simulation was performed using ADS 2011.11 software.

C. Impedance Matching

To maximize the power transferred to the system, the impedance between the antenna and the rectifier should be matched. There are several ways to perform the matching impedance, such as stub and lumped component. The matching impedance was carried out using the Smith Chart simulated by ADS 2011.11, as shown in Figure 4.

III. Results And Discussion

Figure 5 shows the proposed design of the 2.4 GHz energy harvester that consists of an AC power source to represent the receiver antenna, lumped matching impedance, Greinacher RF-DC converter, and 1 kΩ load resistance.

The AC power source was set to a frequency of 2.4 GHz. The impedance is set to 50 Ω as in a manufactured antenna, and the input power is changeable from -20 dBm to 0 dBm.

An impedance matching circuit is required for the RF-to-DC converter to receive all the power received by the antenna. The inductor and capacitor values are obtained by determining the input impedance of the RF-to-DC converter in advance. Figure 6 shows the graph of the S_{11} parameter without impedance matching. S_{11} parameter value obtained at 2.4 GHz is -0.074 dB. As the frequency increases up to 30 GHz, the S_{11} value continues to decrease. That means nearly all received power is reflected to the source.

The matching impedance simulation was generated using ADS 2011.11. The termination on the left represents 50 Ω antenna impedances, and the second termination on the right represents rectifier input impedance. The rectifier input impedance was generated by the software after the component parameters and values were entered. The rectifier input impedance is 3.122 – j 184.211 Ω as shown in Figure 7.

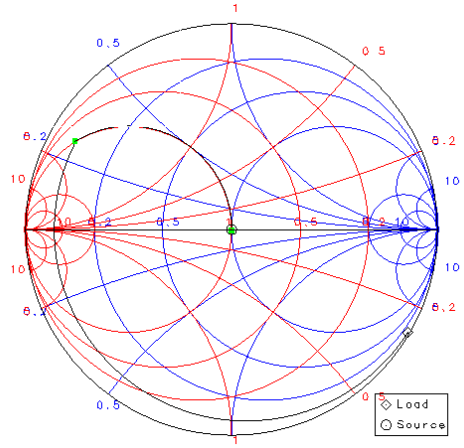

Figure 4. Impedance matching using Smith Chart.

The matching impedance components' value was also generated by ADS 2011.11, which provides the Smith Chart. Figure 8 shows the lumped impedance matching circuit that consists of a 13-nH inductor and a 4.7-pF capacitor connected in L topology.

The impedance matching circuit was then added to the rectifier. The simulation result after using the matching circuit is presented in Figure 9. To be more specific, the S_{11} parameter is captured from 0 up to 3 GHz. At the frequency of 2.4 GHz, the S_{11} parameter obtained is -14.015 dB. This indicates that the circuit is matched at 2.4 GHz.

Figure 10 shows the simulation result of the output voltage at 1 kΩ load. It resulted in 0.257 V_{DC} at 0 dBm input power.

After being simulated, the RFEH was realized on the FR-4 PCB. The PCB thickness is 1.6 mm, and the area of the PCB used is 25 × 30 mm^2. A coin is used as a size comparison, as shown in Figure 11.

Measurements were conducted in two conditions: by directly connecting to the signal generator and by using antennas as a transmitter and a receiver, as shown in Figures 12 and 13.

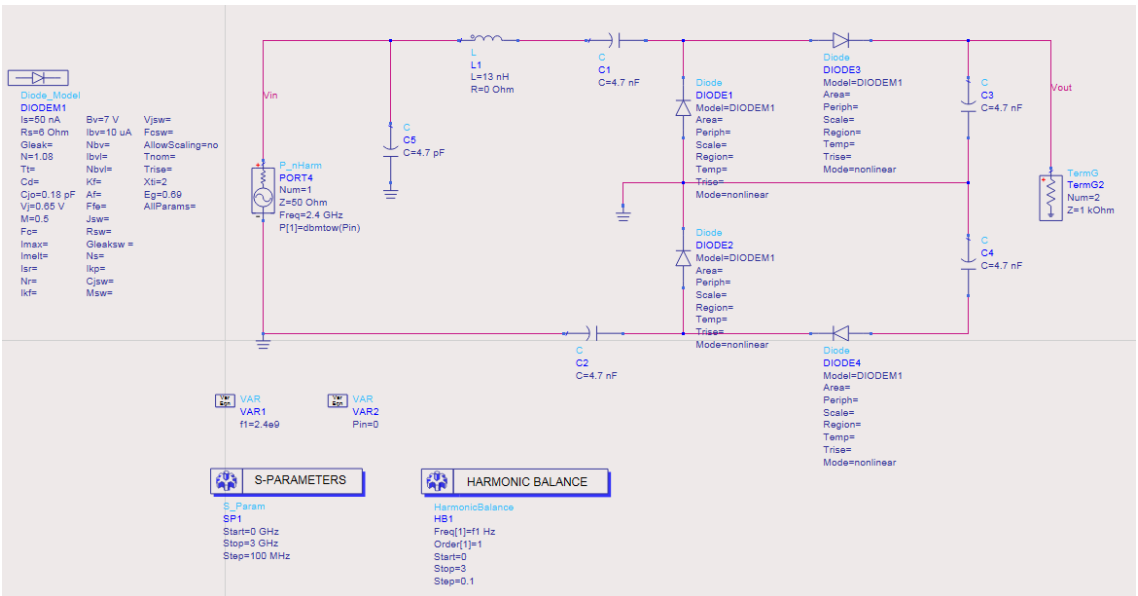

Figure 5. Proposed design of 2.4 GHz RFEH.

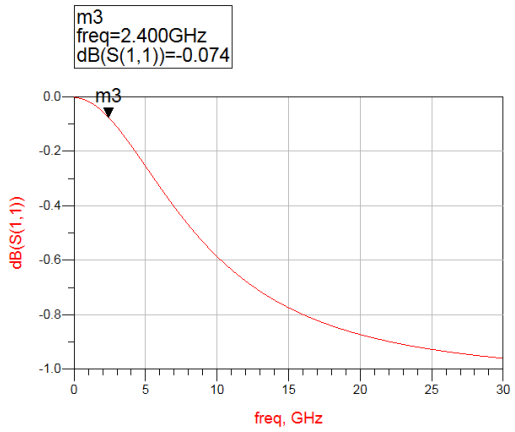

Figure 6. S11 Parameter without matching impedance.

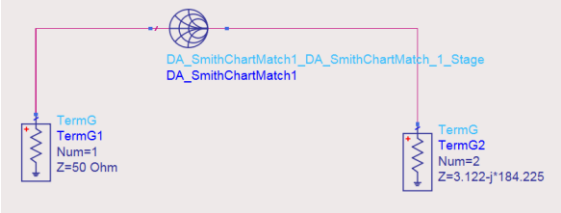

Figure 7. Matching impedance simulation

According to Table 2, there are notable differences in the results. These differences could be due to variations in the parameters of the components, as real PCBs may not be identical to the simulated ones. Imperfect fabrication could also be a contributing factor.

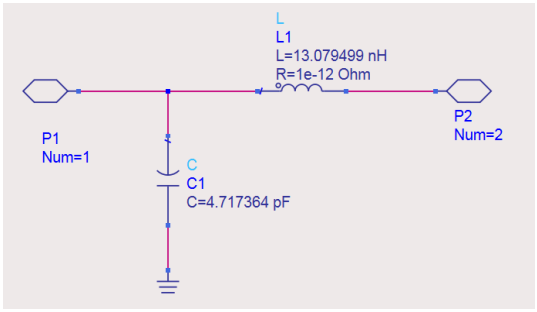

Figure 8. Impedance matching circuit using L topology.

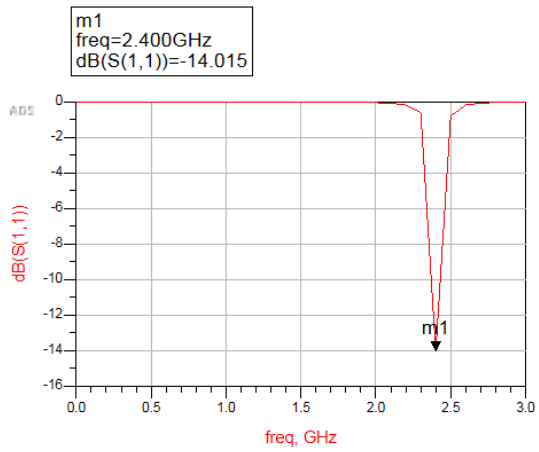

Figure 9. S_{11} Parameter with matching impedance.

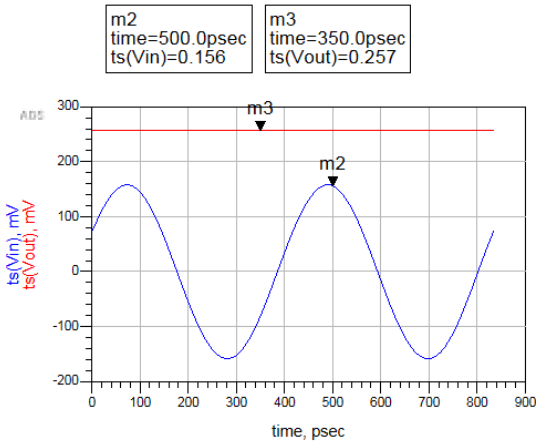

Figure 10. Simulation result of output voltage.

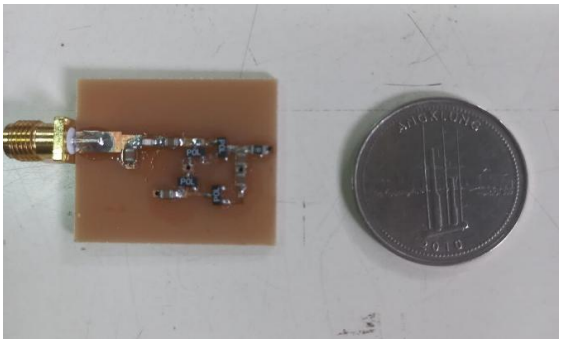

Figure 11. Fabricated RFEH.

The output current was calculated simply using Ohm's law. The peak output current and voltage were obtained at -3 dBm.

Figure 13 shows the experiment setup during RFEH measurement using antennas. An antenna is plugged to the signal generator as a transmitter antenna, and another antenna is installed to the RFEH system as a receiver antenna. The length of both antennas is 10.8 cm, with a gain of 3 dBi. The RFEH is placed at certain distances such as 20 cm, 30 cm, and 50 cm from the transmitter antenna.

From the measurement shown in Table 3, the RFEH able to generate DC voltage at maximum distance of 30 cm. The output voltage is smaller when using an antenna at a distance due to attenuation affected by distance or Free Space Path Loss as (2).

Figure 12. Measurement setup without antenna.

TABLE 2
SIMULATION AND MEASUREMENT RESULTS WITHOUT ANTENNA

P_{in} (dBm)	Simulated V_{out} (mV)	Measured V_{out} (mV)	Current (µA)
-3	205	32.6	32.6
-5	158	19.2	19.2
-10	80	5.2	5.2
-15	37	1.6	1.6
-20	15	0.5	0.5

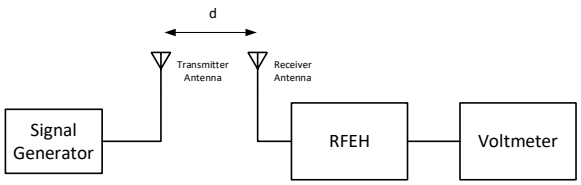

Figure 13. Measurement setup with antenna.

TABLE 3
MEASUREMENT RESULTS AT CERTAIN DISTANCES

Pin (dBm)	Distance (cm)	V_{out} (mV)	Current (µA)
0	20	0.2	0.2
	30	0.1	0.1
	50	0	0
5	20	0.6	0.6
	30	0.1	0.1
	50	0	0

$$FSPL\ (dB) = 20\log_{10}\left(\frac{4\pi df}{c}\right) \quad (2)$$

where:
d = distance between antennas (m)
f = frequency (Hz)
c = light of speed (3×10^8 m/s^2)

The received power can be calculated by (3),

$$P_R = P_T G_T G_R \left(\frac{c}{4\pi df}\right)^2 \quad (3)$$

where:
P_T = Transmitted signal power
G_T = Gain of the transmitting antenna
G_R = Gain of the receiving antenna

The calculation of free space path loss (FSPL) and the received power are displayed in Table 4. In electromagnetic wave transmission, free space loss has a significant impact on signal power as the distance between the transmitter and receiver increases. However, in the near field, the effect of free space loss is smaller compared to the far field. This is because the electromagnetic field at close range remains strong and localized around the source, allowing for more stable and efficient communication over short distances. The reactive near field is calculated using (4).

$$Reactive\ near\ field \leq 0.62\sqrt{\frac{D^3}{\lambda}} \quad (4)$$

where:

TABLE 4
FREE SPACE LOSS AND RECEIVED POWER CALCULATION

Distance (cm)	FSPL (dB)	Power Received (dB)	
		at P_{in} = 0 dBm	at P_{in} = 5 dBm
20	20.06	-20.06	-15.06
30	23.59	-23.59	-18.59
50	28.02	-28.02	-23.02

TABLE 5
PERFORMANCE SUMMARY

Ref	[22]	[23]	[24]	[25]	This work
Topology	Dickson 2 stages	Dickson	Villard	Bridge	Greinacher
Substrate	FR4	RO 4003C	RT/Duroid 6010	N/A	FR4
Receiving antenna type	Patch	2x2 microstrip patch array	Patch (modified shape)	N/A	Dipole
f (GHz)	2.4	2.4	2.45	2.5	2.4
Load (kΩ)	50	50	82	0.5	1
Distance (cm)	N/A	92	N/A	N/A	20
Pin (dBm)	0	27	-20 to 20	0 to 23	5
V_{Out}	5.3 V (on simulation)	1.46 V	6.7 V at 20 dBm	6.94 V at 23 dBm	0.6 mV
I (µA)	N/A	1.9 to 300	N/A	N/A	0.6

D = Antenna dimension (m)
λ = Wavelength (m)

as λ is the speed of light divided by the frequency, we can obtain λ = 12.5 cm. The reactive near field is achieved at a distance of 6.2 cm. The radiating near field can be calculated by (5).

$$Radiating\ near\ field \leq \frac{2D^2}{\lambda} \quad (5)$$

The far field obtained by (6) is the distance further than the radiating near field:

$$Far\ field \geq \frac{2D^2}{\lambda} \quad (6)$$

the far field is achieved when the distance is more than 18.6 cm.

Table 5 summarizes the measurement results of the proposed design compared to the previous studies. The proposed Radio Frequency Energy Harvester (RFEH) offers significant advantages for ultra-low-power Internet of Things (IoT) sensors. The system generated a peak output voltage of 32.6 mV at an input power of -3 dBm when it was directly connected to the signal generator. The calculated output current is 32.6 µA, which is more than sufficient for the sleep mode that requires only 10 µA.

Unlike previous studies, this RFEH utilizes a low load resistance of 1 kΩ and a cost-effective substrate material. The study also measured the output voltage at specific distances with input powers of 0 and 5 dBm. The Greinacher topology was chosen for its simplicity and effectiveness in boosting output voltage while keeping the component count minimal, which is advantageous for compact designs. For future research, the performance could be enhanced by implementing a power management circuit.

IV. CONCLUSION

The proposed design of 2.4 GHz RF Energy Harvester demonstrates the potential to address the

energy needs for ultra-low-power IoT devices. Greinacher topology was chosen as the RF-DC converter with a one kΩ load resistance. The RFEH has -20 dBm sensitivity when directly connected to the signal generator. Peak output voltage and current were obtained at -3 dBm input power. The far-field experiment was performed by attaching a receiver antenna to the RFEH and measuring at certain distances.

DECLARATIONS

Conflict of Interest

The authors have declared that no competing interests exist.

CRediT Authorship Contribution

Farrah Vauzia: Funding Acquisition, Conceptualization, Visualization, Writing-Original Draft, Methodology; Enceng Sulaeman: Software, Formal Analysis, Validation; Yana Taryana: Resources, Data Curation, Investigation, Writing-Reviewing and Editing.

Funding

Research reported in this publication was supported by Pusat Penelitian dan Pengabdian Kepada Masyarakat Politeknik Negeri Bandung under grant number B/6.35/PL1.R7/PG.00.03/2024.

REFERENCES

[1] Misra, G. Das, and D. Das, "An iot based wireless energy harvesting using efficient voltage doubler stages in a rf to dc converter," *2018 4th International Conference on Computing Communication and Automation, ICCCA 2018*, pp. 1–5, 2018, doi: 10.1109/CCAA.2018.8777712.

[2] A. S. Thangarajan *et al.*, "Static: low frequency energy harvesting and power transfer for the internet of things," *Frontiers in Signal Processing*, vol. 1, no. January, pp. 1–13, 2022, doi: 10.3389/frsip.2021.763299.

[3] H. H. Ibrahim *et al.*, "Radio frequency energy harvesting technologies: a comprehensive review on designing, methodologies, and potential applications," *Sensors*, vol. 22, no. 11, 2022, doi: 10.3390/s22114144.

[4] T. Sondej and B. Mariusz, "Ultra-low-power sensor nodes for real-time synchronous and high-accuracy timing wireless data acquisition," *Sensors 2024*, vol. 24, p. 4871, 2024, doi: https://doi.org/10.3390/s24154871.

[5] F. Mazunga and A. Nechibvute, "Ultra-low power techniques in energy harvesting wireless sensor networks: recent advances and issues," *Sci Afr*, vol. 11, p. e00720, 2021, doi: 10.1016/j.sciaf.2021.e00720.

[6] D. Tokmakov, S. Asenov, and S. Dimitrov, "Research and development of ultra-low power lorawan sensor node," 2019. doi: 10.1109/ET.2019.8878674.

[7] J. Henkel, S. Pagani, H. Amrouch, L. Bauer, and F. Samie, "Ultra-low power and dependability for iot devices (special session paper)," Mar. 2017. [Online]. Available: https://www.researchgate.net/publication/312214220

[8] T. Caroff *et al.*, "Ultra low power wireless multi-sensor platform dedicated to machine tool condition monitoring," in *30th International Conference on Flexible Automation and Intelligent Manufacturing (FAIM2021)*, 2020, pp. 296–301.

[9] L. J. Gabrillo, M. G. Galesand, and J. A. Hora, "Enhanced rf to dc converter with lc resonant circuit," in *IOP Conf Ser Mater Sci Eng*, 2015, vol. 79, no. 1. doi: 10.1088/1757-899X/79/1/012011.

[10] M. Basim *et al.*, "A highly efficient rf-dc converter for energy harvesting applications using a threshold voltage cancellation scheme," *Sensors*, vol. 22, no. 7, 2022, doi: 10.3390/s22072659.

[11] M. A. Gozel, M. Kahriman, and O. Kasar, "Design of an efficiency-enhanced greinacher rectifier operating in the gsm 1800 band by using rat-race coupler for rf energy harvesting applications," *International Journal of RF and Microwave Computer-Aided Engineering*, 2019, doi: 10.1002/mmce.21621.

[12] P. Kundu, J. Acharjee, and K. Mandal, "Design of an efficient rectifier circuit for rf energy harvesting system to cite this version : hal id : hal-01592486 design of an efficient rectifier circuit for rf energy harvesting system," *International Journal of Advanced Engineering and Management*, vol. 2, pp. 94–97, 2017.

[13] P. Saffari, A. Basaligheh, and K. Moez, "An rf-to-dc rectifier with high efficiency over wide input power range for rf energy harvesting applications," *IEEE Transactions on Circuits and Systems I: Regular Papers*, vol. 66, no. 12, pp. 4862–4875, 2019, doi: 10.1109/TCSI.2019.2931485.

[14] I. D. Bougas, M. S. Papadopoulou, A. D. Boursianis, S. Nikolaidis, and S. K. Goudos, "Dual-band rectifier circuit design for iot communication in 5g systems," *Technologies (Basel)*, vol. 11, no. 2, pp. 1–15, 2023, doi: 10.3390/technologies11020034.

[15] L. M. Borges, R. Chávez-Santiago, N. Barroca, F. J. Velez, and I. Balasingham, "Radio-frequency energy harvesting for wearable sensors," *Healthc Technol Lett*, vol. 2, no. 1, pp. 22–27, 2015, doi: 10.1049/htl.2014.0096.

[16] E. Sulaeman and N. Wardah, "Design of an RF Rectifier for Electromagnetic Energy Harvesting in the 900 MHz GSM Band," (in Indonesian), *JTERA (Jurnal Teknologi Rekayasa)*, vol. 4, no. 2, p. 253, 2019, doi: 10.31544/jtera.v4.i2.2019.253-260.

[17] M. Koohestani, J. Tissier, and M. Latrach, "A miniaturized printed rectenna for wireless rf energy harvesting around 2.45 ghz," *AEU - International Journal of Electronics and Communications*, vol. 127, no. June, 2020, doi: 10.1016/j.aeue.2020.153478.

[18] D. G. Molinos, H. Solar, A. Beriain, and R. Berenguer, "Voltage multiplier topologies comparison for uhf rfid applications," 2020. doi: 10.1109/DCIS51330.2020.9268624.

[19] F. Sari and Y. Uzun, "A comparative study: voltage multipliers for rf energy harvesting system," *Communications Faculty of Sciences University of Ankara Series A2-A3 Physical Sciences and Engineering*, vol. 61, no. 1, pp. 12–23, 2019, doi: 10.33769/aupse.469183.

[20] V. B. Tom and S. Michiel, *CMOS Integrated Capacitive DC-DC Converters*. New York, 2013.

[21] K. K. A. Devi, M. D. Norashidah, C. K. Chakrabarty, and S. Sadasivam, "Design of an rf-dc conversion circuit for energy harvesting," in *International Conference on Electronic Devices, Systems, and Applications*, 2012, pp. 156–161. doi: 10.1109/ICEDSA.2012.6507787.

[22] N. U. Khan and F. U. Khan, "RF energy harvesting for portable biomedical devices," Nov. 2019. doi: 10.1109/INMIC48123.2019.9022759.

[23] C. Shekhar and S. Varma, "An optimized 2.4 ghz rf energy harvester for energizing low-power wireless sensor platforms," *Journal of Circuits, Systems and Computers*, vol. 28, no. 6, 2019, doi: 10.1142/S0218126619501044.

[24] W. Ali, H. Subbyal, L. Sun, and S. Shamoon, "Wireless energy harvesting using rectenna integrated with voltage multiplier circuit at 2.4 ghz operating frequency," *Journal of Power and Energy Engineering*, vol. 10, no. 03, pp. 22–34, 2022, doi: 10.4236/jpee.2022.103002.

[25] P. Kundu, J. Acharjee, and K. Mandal, "Design of an efficient rectifier circuit for rf energy harvesting system to cite this version : hal id : hal-01592486 design of an efficient rectifier circuit for rf energy harvesting system," *International Journal of Advanced Engineering and Management*, vol. 2, pp. 94–97, 2017, [Online]. Available: https://ijoaem.org/00204-24.